ARTICLE

Precision Motion Control of Hydraulic Actuator Using Adaptive Back-Stepping Sliding Mode Controller

Zhenshuai Wan[1,2,*], Longwang Yue[2], Yanfeng Wang[2] and Pu Zhao[2]

[1]Henan Key Laboratory of Superhard Abrasives and Grinding Equipment, Henan University of Technology, Zhengzhou, 450001, China

[2]School of Mechanical and Electrical Engineering, Henan University of Technology, Zhengzhou, 450001, China

*Corresponding Author: Zhenshuai Wan. Email: wanzhenshuai@haut.edu.cn

ABSTRACT

Hydraulic actuators are highly nonlinear when they are subjected to different types of model uncertainties and dynamic disturbances. These unfavorable factors adversely affect the control performance of the hydraulic actuator. Although various control methods have been employed to improve the tracking precision of the dynamic system, optimizing and adjusting control gain to mitigate the hydraulic actuator model uncertainties remains elusive. This study presents an adaptive back-stepping sliding mode controller (ABSMC) to enhance the trajectory tracking precision, where the virtual control law is constructed to replace the position error. The adaptive control theory is introduced in back-stepping controller design to compensate for the model uncertainties and time-varying disturbances. Based on Lyapunov theory, the finite-time convergence of the position tracking errors is proved. Furthermore, the effectiveness of the developed control scheme is conducted via extensive comparative experiments.

KEYWORDS

Hydraulic actuator; back-stepping control; adaptive control; model uncertainties

1 Introduction

In virtues of fast response, high power-to-weight ratio, as well as larger driving force, hydraulic actuators have been widely used in many equipment [1], e.g., robotic actuators, rolling machines, and load simulators, in which good dynamic response and high accuracy tracking performance are crucial [2–5]. Meanwhile, various model uncertainties and dynamic disturbances such as frictions, unknown payloads, backlash, and unmodeled dynamics widely exist in hydraulic actuators, adversely affecting their control performance [6–9]. Due to the increasing interest in high-precision control, reducing the influence of external load disturbance and parameter change is a key goal for hydraulic servo system controller design.

So as to retain the satisfactory control performance of hydraulic actuators, several progressive control methods have been developed, such as adaptive control [10–12], robust control [13–16], back-stepping control [17–20] and sliding mode control (SMC) [21–24]. Adaptive control can reach a good

position by tracking the controller under parameter uncertainties utilizing the online learning control law. However, the parameter convergence of the adaptive law can only be realized under continuous excitation, which is too stringent to be satisfied in practice. Guo et al. [25] proposed an adaptive controller with improved parameter convergence to achieve the high-performance trajectory tracking control of a hydraulic servo system, where the composite learning scheme is driven by both tracking and prediction error. Back-stepping control has been successfully utilized to deal with the nonlinear system. Then, Guo et al. [26] proposed a back-stepping control scheme with an extended-state-observer (ESO) to handle the load disturbance and uncertain nonlinearity of the electro-hydraulic system, where the ESO is presented to estimate the external disturbance and modeling uncertainty. In order to solve the discontinuity problem of traditional SMC, the continuous saturation function rather than the discontinuous sign function is adopted in the controller design procedure [27–29]. Although the tracking error of the abovementioned can be guaranteed to be bounded, the asymptotic tracking performance is lost. The high-order SMC can obtain asymptotic tracking and controller continuity, but the controller design needs information on the derivatives of sliding mode variables [30]. However, the sliding mode variable derivative is often considered unknown in practice, so it is not easy to implement in real systems [31]. Super-twisting SMC can avoid the problems above, but the gain of the controller must be artificially set, which is conservative to some certain extent [32]. With the motivation discussed above, the adaptive back-stepping sliding mode controller (ABSMC) control scheme is proposed to deal with various modeling uncertainties and external disturbances of the hydraulic actuator. Based on the system model information, the adaptive law is added to the traditional SMC to improve the system's servo controller precision. The main innovations of this study are summarized as follows. 1) The nonlinear model of the hydraulic actuator considering model uncertainties and dynamic disturbances is constructed. 2) The proposed control scheme improves the robustness and disturbance rejection performance by utilizing the back-stepping and SMC. 3) The faster convergence chattering suppression is validated by different work conditions under uncertainties.

The paper is structured as follows: The dynamic model is formulated in Section 2. Section 3 proposes the SMC design with adaptive control law, where the system stability analysis is also provided. Comparative studies are discussed in Section 4, where the superiority of the ABSMC is described in comparison to the other controllers. Finally, conclusions are drawn in Section 5.

2 Dynamic Model and Problem Formulation

In this section, the dynamic characteristics of the hydraulic actuator are provided, and the related control problems are formulated. Fig. 1 shows the schematic diagram of the hydraulic actuator, comprised of a double-acting hydraulic cylinder, servo valve, electric motor, relief valve, and accumulator. As a conversion device, the hydraulic pump converts the motor's electric energy into the hydraulic energy of oil. The servo valve provides the oil pressure to the hydraulic cylinder for controlling the piston's movement. The variable pressure of incompressible fluid hinders the precise control of the actuator. An accurate mathematical model is the first step of controller design, so the hydraulic actuator's dynamic model is performed below.

The flow pressure relation of servo valve is described as follows [33]:

$$Q_L = C_d w x_v \sqrt{\frac{P_s - \text{sgn}(x_v) P_L}{\rho}} \tag{1}$$

where Q_L is load flow, C_d is discharge coefficient, w is the area gradient of the servo valve, P_s is supply pressure, P_L is load pressure, and ρ is hydraulic oil density.
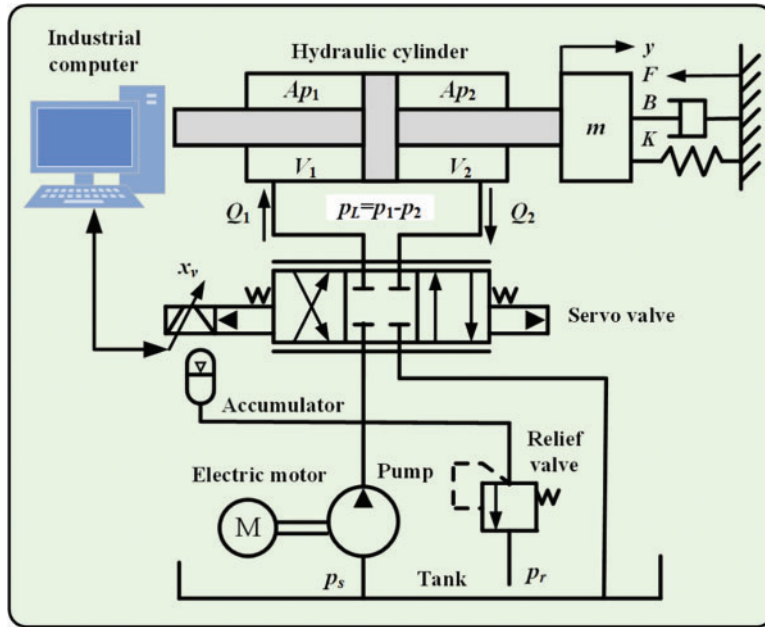
Figure 1: Scheme diagram of the hydraulic actuator

Because the servo valve dynamic characteristics are faster than the rest of the system, the relationship between input voltage and spool displacement is given by

$$x_v = k_{sv}u \tag{2}$$

where k_{sv} is the torque motor gain, and u is the input voltage of the torque motor.

The load pressure dynamics of the hydraulic actuator are capable to be expressed as follows:

$$\frac{V_t}{4\beta_e}\dot{P}_L = -A\dot{y} - C_tP_L + Q_L \tag{3}$$

where V_t is the total control volume of the cylinder chamber, β_e is the effective bulk modulus, A is the actuator ram area, and C_t is the total leakage coefficient.

Based on the Newton's second law, the load motion can be described as follows:

$$P_LA = m\ddot{y} + B\dot{y} + Ky + f \tag{4}$$

where m is the load mass, B is the actuator ram area, K is the viscous damping coefficient of hydraulic oil, and f is the external load of the system.

The state variables are defined as $[x_1, x_2, x_3]^T = [y, \dot{y}, \ddot{y}]$, and then the state space model of the hydraulic actuator is described by

$$\begin{cases} \dot{x}_1 = x_2 \\ \dot{x}_2 = x_3 \\ \dot{x}_3 = -a_1x_2 - a_2x_3 + b_0u + F \end{cases} \tag{5}$$

where $a_1 = -K/m - (4A^2\beta_e)/(mV_t)$, $a_2 = -B/m$, $F = -(4A\beta_eC_tP_L)/(mV_t) - \dot{f}/m$,

$b_0 = (4A\beta_eC_dwk_{sv}\sqrt{P_s - \text{sgn}(x_v)P_L})/(mV_t\sqrt{\rho})$.

The total uncertainty F is bounded, satisfying the following condition [34]:

$$|F| \leq \overline{F} \tag{6}$$

where $\overline{F}$ is a real value.

3 Controller Design

The objective of controller design is to construct an adaptive control strategy such that the cylinder displacement x_1 tracks the desired trajectory x_d accurately under model uncertainties and dynamic disturbances.

3.1 Back-Stepping Sliding Mode Controller

The position tracking error and its time derivative are defined as follows:

$$z_1 = x_1 - x_d \tag{7}$$

$$\dot{z}_1 = x_2 - \dot{x}_d \tag{8}$$

The first Lyapunov function is defined as follows:

$$V_1 = \frac{1}{2}z_1^2 \tag{9}$$

Define

$$x_2 = -c_1 z_1 + \dot{x}_d + z_2 \tag{10}$$

where c_1 is a positive constant.

Then, the virtual control law z_2 is selected as follows:

$$z_2 = x_2 - \dot{x}_d + c_1 z_1 \tag{11}$$

The time derivative of the Lyapunov function V_1 is given by

$$V_1 = -c_1 z_1^2 + z_1 z_2 \tag{12}$$

Clearly, if $z_2 = 0$, then $\dot{V}_1 \leq 0$ and the first subsystem is stable.

The second Lyapunov function is defined as follows:

$$V_2 = V_1 + \frac{1}{2}z_2^2 \tag{13}$$

The time derivative of V_2 is

$$\dot{V}_2 = \dot{V}_1 + z_2 \dot{z}_2 = -c_1 z_1^2 + z_1 z_2 + z_2 (x_3 + c_1 \dot{z}_1 - \ddot{x}_d) \tag{14}$$

Define

$$x_3 = -c_1 \dot{z}_1 + \ddot{x}_d - z_1 - c_2 z_2 + z_3 \tag{15}$$

where c_2 is a positive constant.

The virtual control law z_3 is selected as follows:

$$z_3 = x_3 + c_2 z_2 + c_1 \dot{z}_1 + z_1 - \ddot{x}_d \tag{16}$$

Then Eq. (14) can be written as follows:

$$\dot{V}_2 = -c_1 z_1^2 - c_2 z_2^2 + z_2 z_3 \tag{17}$$

The sliding surface is defined as follows:

$$\sigma = k_1 z_1 + k_2 z_2 + z_3 \tag{18}$$

The third Lyapunov function is selected as follows:

$$V_3 = V_2 + \frac{1}{2}\sigma^2 \tag{19}$$

Taking the derivative of Eq. (19) with respect to time gives

$$\begin{aligned}
\dot{V}_3 &= \dot{V}_2 + \sigma\dot{\sigma} \\
&= -c_1 z_1^2 - c_2 z_2^2 + z_2 z_3 + \sigma\left(k_1 \dot{z}_1 + k_2 \dot{z}_2 + \dot{z}_3\right) \\
&= -c_1 z_1^2 - c_2 z_2^2 + z_2 z_3 + \sigma\left(k_1 \dot{z}_1 + k_2 \dot{z}_2 \right. \\
&\quad \left. -a_1 x_2 - a_2 x_3 + b_0 u + F + c_1 \ddot{z}_1 + c_2 \dot{z}_2 + \dot{z}_1 - \dddot{x}_d\right)
\end{aligned} \tag{20}$$

Given the dynamic system, the control law is designed as follows:

$$\begin{aligned}
u &= \frac{1}{b_0}\left(-k_1 \dot{z}_1 - k_2 \dot{z}_2 + a_1 x_2 + a_2 x_3 - \overline{F}\,\mathrm{sgn}\,(\sigma) \right. \\
&\quad \left. -c_1 \ddot{z}_1 - c_2 \dot{z}_2 - \dot{z}_1 + \overline{x}_d - h\left(\sigma + \beta\,\mathrm{sgn}\,(\sigma)\right)\right)
\end{aligned} \tag{21}$$

where h and β are positive constants.

Substituting Eq. (21) into Eq. (20) leads for

$$\begin{aligned}
\dot{V}_3 &= -c_1 z_1^2 - c_2 z_2^2 + z_2 z_3 - h\sigma^2 - h\beta|\sigma| + F\sigma - \overline{F}|\sigma| \\
&\leq -c_1 z_1^2 - c_2 z_2^2 + z_2 z_3 - h\sigma^2 - h\beta|\sigma|
\end{aligned} \tag{22}$$

Selecting the matrix $\mathbf{Q}$ as follows:

$$\mathbf{Q} = \begin{bmatrix} hk_1^2 + c_1 & hk_1 k_2 & hk_1 \\ hk_1 k_2 & c_2 + k_2^2 & hk_2 - 1/2 \\ hk_1 & hk_2 - 1/2 & h \end{bmatrix} \tag{23}$$

Define $\mathbf{Z}^T = [z_1, z_2, z_3]$, then

$$\begin{aligned}
\mathbf{Z}^T \mathbf{Q} \mathbf{Z} &= [z_1, z_2, z_3] \begin{bmatrix} hk_1^2 + c_1 & hk_1 k_2 & hk_1 \\ hk_1 k_2 & c_2 + k_2^2 & hk_2 - 1/2 \\ hk_1 & hk_2 - 1/2 & h \end{bmatrix} \begin{bmatrix} z_1 \\ z_2 \\ z_3 \end{bmatrix} \\
&= c_1 z_1^2 + c_2 z_2^2 - z_2 z_3 + h\sigma^2
\end{aligned} \tag{24}$$

If the $\mathbf{Q}$ is a positive definite matrix, then

$$V_3 \leq -\mathbf{Z}^T \mathbf{Q} \mathbf{Z} - h\beta|\sigma| \leq 0 \tag{25}$$

in which,

$$|\mathbf{Q}| \leq c_1 h\left(k_2 + c_2\right) - \left(c_1 + hk_1^2\right)/4 \tag{26}$$

By choosing the appropriate value for h, c_1, c_2, k_1, k_2, and $|Q| > 0$, then

$$\dot{V}_3 \le 0 \tag{27}$$

Based on LaSalle's invariance principle, if $\dot{V}_3 \equiv 0$, then $z_3 \equiv 0$, $\sigma \equiv 0$. As $t \to 0$, then $z \to 0$, $\sigma \to 0$ and $x_1 \to x_d$.

3.2 Adaptive Control Law Design

The controller mentioned above design is based on the assumption that the bound of the uncertainty F is known. Uncertainty and external disturbance are usually unknown in practical situations, so the F is difficult to determine. Given this condition, an adaptive control law is developed to estimate the F. It is assumed that the total uncertainty items change slowly then $\dot{F} = 0$.

The estimation error is derived as follows:

$$\tilde{F} = F - \hat{F} \tag{28}$$

where $\hat{F}$ is the estimation of F.

The Lyapunov function candidate is defined as follows [35]:

$$V_4 = V_3 + \frac{1}{2\gamma}\tilde{F}^2 \tag{29}$$

where γ is a positive constant.

The time derivative of V_4 is

$$\dot{V}_4 = \dot{V}_3 - \frac{1}{\gamma}\tilde{F}\dot{\hat{F}} = \dot{V}_3 - \frac{1}{\gamma}\tilde{F}\left(\dot{\hat{F}} + \gamma\sigma\right) \tag{30}$$

The adaptive control law is designed as follows:

$$\dot{\hat{F}} = -\gamma\sigma \tag{31}$$

Thus, the ABSMC is presented as follows:

$$u = \frac{1}{b_0}\left(-k_1\dot{z}_1 - k_2\dot{z}_2 + a_1 x_2 + a_2 x_3 - \hat{F}\right.$$
$$\left. -c_1\ddot{z}_1 - c_2\dot{z}_2 - \dot{z}_1 + \dddot{x}_d - h\left(\sigma + \beta\,\mathrm{sgn}\left(\sigma\right)\right)\right) \tag{32}$$

Substituting Eq. (31) into Eq. (30) leads for

$$\dot{V}_4 = -c_1 z_1^2 - c_2 z_2^2 + z_2 z_3 - h\sigma^2 - h\beta|\sigma|$$
$$= -\mathbf{Z}^T \mathbf{Q}\mathbf{Z} - h\beta|\sigma|$$
$$\le 0 \tag{33}$$

Based on the Lyapunov-Like Lemma, the hydraulic actuator is globally asymptotically stable by adopting adaptive sliding mode control law. Hence, the hydraulic actuator can accurately track the reference trajectory at the desired position. For ease of understanding of the proposed controller, its block diagram is provided as shown in Fig. 2. To ensure the robustness of the hydraulic actuator to uncertainty and interference, the sliding surface is introduced into the back-stepping control. In addition, the adaptive law is adopted to estimate the model uncertainties.
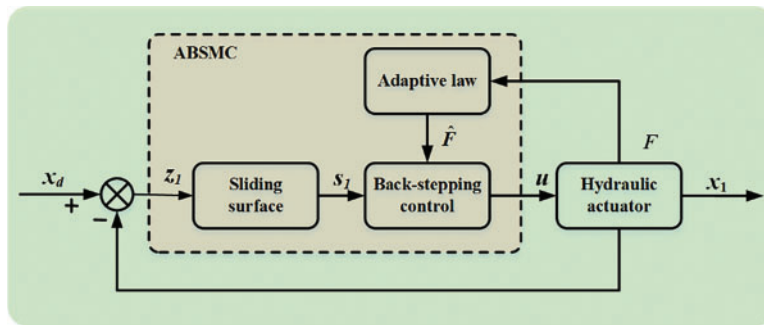
Figure 2: Block diagram of the proposed controller

4 Comparative Studies

To illustrate the effectiveness of the developed control scheme, a hydraulic actuator experimental platform is set up, as shown in Fig. 3. It consists of hydraulic actuator, a servo valve whose flow rate is 75 L/min, a sensor system including position sensor and pressure, a signal conditioner working signal conversion and filtering, a control system that includes host computer as well as target computer connecting signal by TCP/IP, and a real-time control software with 16-bit A/D card well as 16-bit D/A card. The hydraulic actuator displacement is driven by a servo valve control signal, regulated by a signal conditioner. Feedback signals, including position and pressure, are collected by the A/D board in real time and sent to a computer for a closed feedback system. The sample time of experimental equipment is 1 ms. The specificparameters of the system are displayed in Table 1. In this study, three controllers are compared.
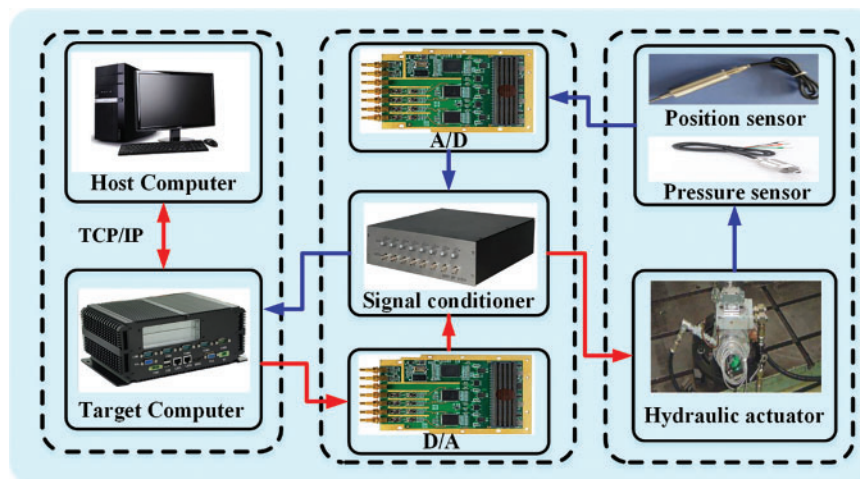

Figure 3: Experimental platform of hydraulic actuator system

ABSMC: The parameters of ABSMC are designed as $h = 200$, $\beta = 0.8$, $c_1 = 300$, $c_2 = 400$, $k_1 = 80$, $k_1 = 60$, and the adaptive control law $\gamma = 0.1$. These controller gains are determined to be optimal parameters after many trials to make a tradeoff between the transient performance and the steady-state performance. The symbolic function is replaced by a saturation function to reduce signal buffeting.

Table 1: The parameters of experimental system

Parameters	Unit	Value	Parameters	Unit	Value
P_s	Pa	1.3×10^8	K	N/m	6×10^3
m	kg	200	β_e	N/m^2	5×10^8
A	m^2	3.14×10^{-4}	C_t	m^4·s/kg	4×10^{-3}
B	N·s/m	1.2×10^3	ρ	kg/m^3	900
k_{sv}	m/V	1.2×10^{-5}	u	V	24
w	–	5×10^{-3}	C_d	–	0.6

SMC: The control law is set as $u = (a_1 x_2 + a_2 x_3 + \dddot{x}_d - k_1 z_1 - k_2 z_3 - k_3 \text{sign}(\sigma))$, where $k_1 = 3000$, $k_2 = 1000$, and $k_3 = 160$.

PID (Proportion Integration Differentiation): The PID parameters are designed as $K_p = 40$, $K_i = 1$, and $K_d = 0.2$ using an intelligent optimization algorithm. The above design parameters have considered the system's steady-state and transient performance.

The three controllers are first tested for sinusoidal motion trajectory $y = 60 \sin(2\pi t)$ mm. The tracking result and errors are compared in Figs. 4 and 5, respectively. The tracking trajectory nearly overlaps the desired ones, and the tracking errors are bounded and stable. Compared to PID, SMC improves the tracking precision to some extent. In addition, the tracking error of ABSMC is smaller than that of SMC. This is because the designed adaptive control law deals with the parametric uncertainties and dynamic disturbance well. The ABSMC achieves the smallest tracking error by employing the proposed control scheme, with an almost 80% reduction for the maximum tracking error. The compared control input of three controllers is shown in Fig. 6. All the control inputs are continuous and bounded, and PID produces the largest control amplitude and violently violent fluctuation. In addition, the chattering level of ABSMC is lower than that of SMC, which is essential to actuators in practice applications. The disturbance estimation and adaptive control law curve are displayed in Fig. 7, where the disturbance signal is set as $y = 12 \sin(2\pi t)$ mm. The unknown dynamics are estimated by the proposed estimator, and the adaptive control law tends to be stable after a short fluctuation. To further show the effectiveness of ABSMC, the sinusoidal signals with different amplitudes and frequencies are studied. The corresponding experimental results are shown in Fig. 8, which indicates that the error indices increase as the amplitude of sinusoidal trajectories increases from 75 to 90 mm. In contrast, the lower the reference signal frequency, the smaller the tracking error indices.
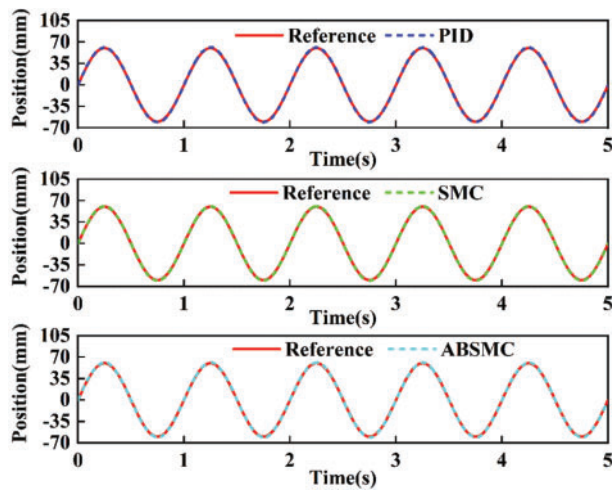
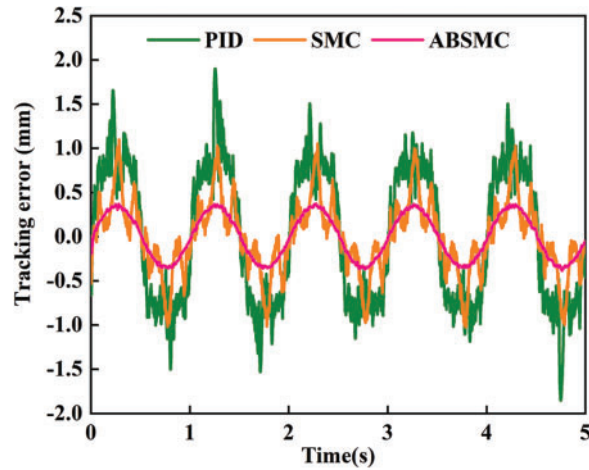**Figure 4:** Tracking trajectory of sinusoidal motion

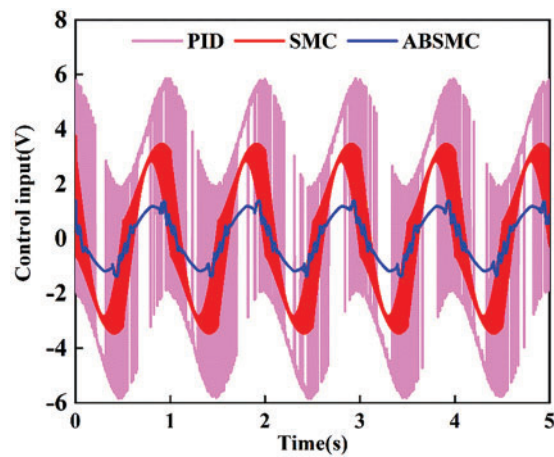**Figure 5:** Tracking error of sinusoidal motion

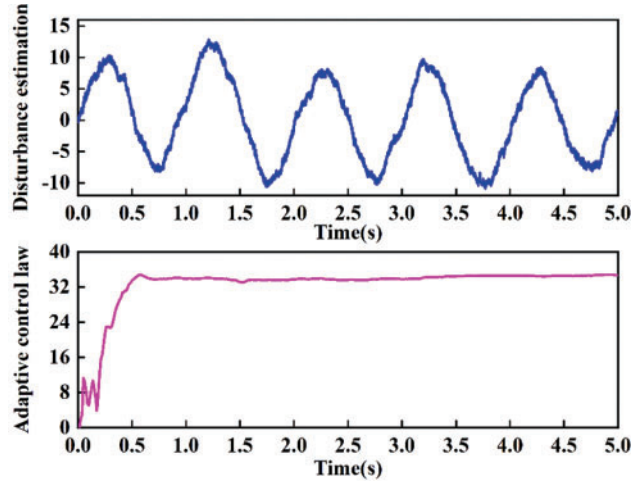**Figure 6:** Control input of sinusoidal motion

Figure 7: Disturbance of sinusoidal motion estimation and adaptive control law curve
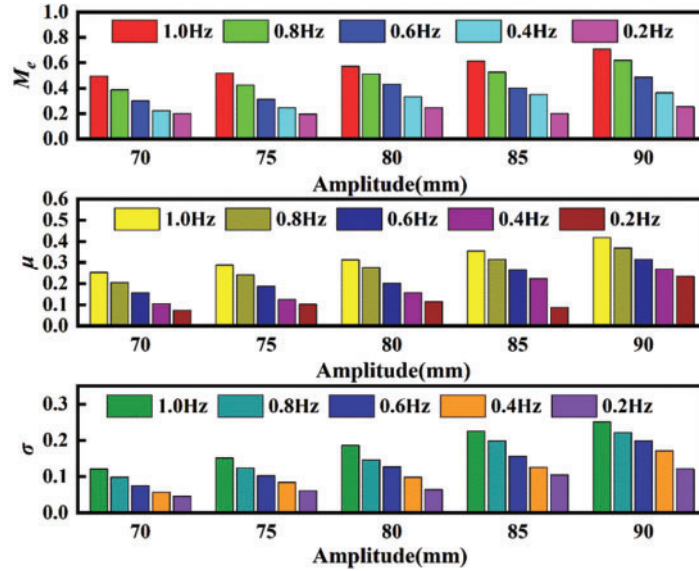

Figure 8: Comparison of performance indices for different reference signals

For the quantitative analysis of the control performance of different controllers, the maximum absolute error M_e, the mean absolute error μ_e, and the average standard absolute error σ_e are defined as

$$\begin{cases} M_e = \max_{i=1,\cdots N} |e_1(i)| \\ \mu_e = \dfrac{1}{N}\sum_{i=1}^{N} |e_1(i)| \\ \sigma_e = \sqrt{\dfrac{1}{N}\sum_{i=1}^{N} [|e_1(i)| - \mu_e]^2} \end{cases} \tag{34}$$

where e_1 is the position tracking error and N is the number of datasets.

The performance indices of sinusoidal motion are listed in Table 2. The proposed ABSMC gives smaller indices value than the other two controllers. The SMC produces better control performance than the PID. Compared to the other two controllers, the σ_e of ABSMC is the least, which means the chattering is also the least among the abovementioned three controllers. This is because the adaptive control law has less noise sensitivity. Namely, the proposed ABSMC obtains the best tracking performance.

Table 2: Performance indices of sinusoidal motion

Indices	M_e	μ_e	σ_e
PID	1.9002	0.7208	0.3014
SMC	1.2924	0.3720	0.2824
ABSMC	0.3752	0.2265	0.1045

To further test the control performance of the proposed ABSMC method, a multifrequency-sinusoidal motion trajectory $y = 60 \sin(2\pi t) + 30 \sin(5\pi t)$ mm is applied. The tracking trajectory and tracking error of multifrequency-sinusoidal motion are depicted in Figs. 9 and 10, respectively. One can find that the tracking performance of PID is less than that of the other two control methods. Although some chatter exists in ABSMC, the control input is reduced compared to SMC. Fig. 11 shows their comparative control input. The control input is smoother than that of SMC and PID, which helps reduce chattering and improve control performance. The performance indices of multifrequency-sinusoidal motion are collected in Table 3. The M_e of the ABSMC is 12.0252 mm, smaller than that of SMC (9.6166 mm) and PID control (4.6913 mm). It indicates that the proposed ABSMC can obtain tracking accuracy at a satisfactory level.
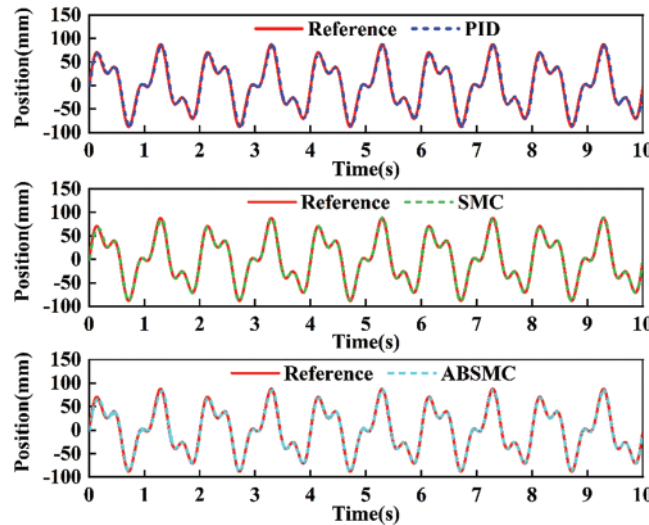

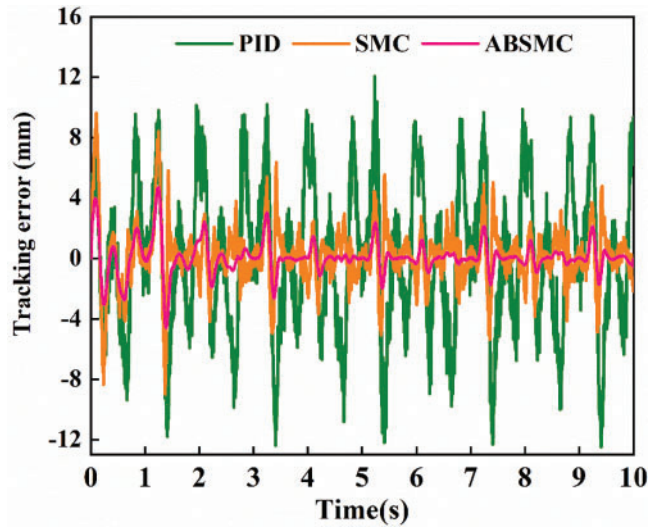**Figure 9:** Tracking trajectory of multifrequency-sinusoidal motion

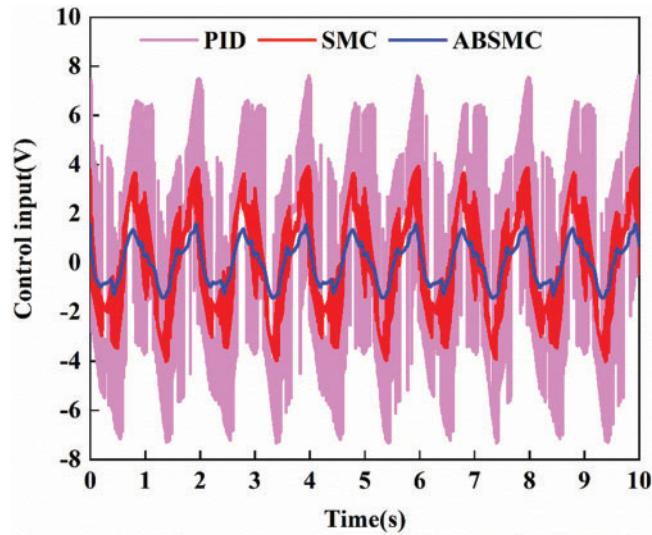**Figure 10:** Tracking error of multifrequency-sinusoidal motion

Figure 11: Control input of multifrequency-sinusoidal motion

Table 3: Performance indices of multifrequency-sinusoidal motion

Indices	M_e	μ_e	σ_e
PID	12.0252	3.9661	2.8385
SMC	9.6166	1.3385	1.5291
ABSMC	4.69133	0.6366	0.8852

The results of trajectory tracking and tracking error of quasi-sinusoidal motion $y = 30$ arctan(sin($20\pi t$)) $[1-\exp(-6t)]$ are shown in Figs. 12 and 13, respectively. The trajectory tracking

performance of ABSMC is, again, better than that of the other two controllers. In addition, PID and SMC have higher peak errors than the ABSMC when the actuator changes its direction. The corresponding performance indices of quasi-sinusoidal motion are listed in Table 4. The ABSMC performs better than the classical PID and SMC of its adaptive control law. Although the SMC also uses the sliding theory, its tracking performance is worse than that of the SMC. This verifies the superiority of the adaptive law in the ABSMC controller.
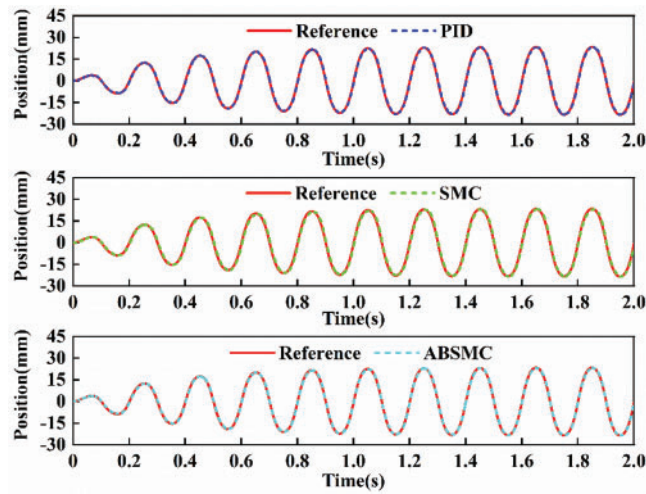

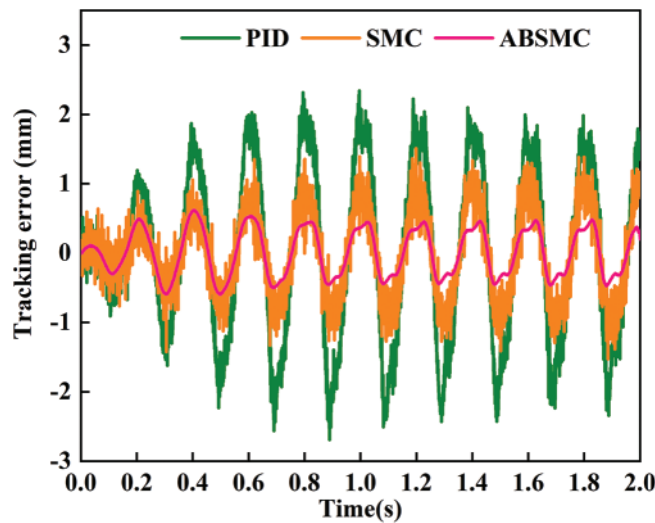**Figure 12:** Tracking trajectory of quasi-sinusoidal motion

Figure 13: Tracking error of quasi-sinusoidal motion

Table 4: Performance indices of quasi-sinusoidal motion

Indices	M_e	μ_e	σ_e
PID	2.3402	1.0684	0.6278
SMC	1.6755	0.5818	0.3678
ABSMC	0.6191	0.3038	0.1466

Fig. 14 shows the comparison results of stochastic signal with an amplitude of 5 m/s^2 and frequency of 1–30 Hz. The tracking precision of the acceleration response under the PID controller is relatively poor. Although SMC improves the accuracy of the acceleration waveform, the tracking effect is not improved. After the ABSMC is adopted, the precision of waveform reproduction is enhanced, and the reference acceleration signal is tracked well. The acceleration response under the EI Centro seismic signal is shown in Fig. 15. The tracking performance of SMC is better than that of PID controller, while the tracking performance of ABSMC is better than that of SMC. That is to say, the acceleration response based on ABSMC has better tracking accuracy than PID and SMC for random and seismic signals.
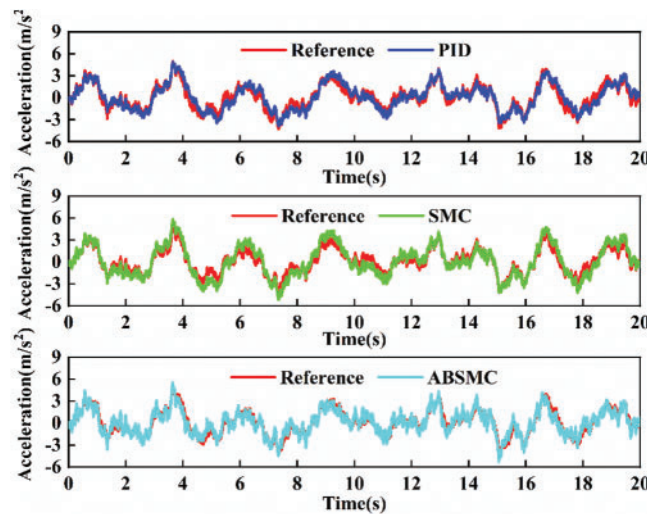

Figure 14: Tracking trajectory of stochastic acceleration motion

Fig. 16 compares the performance indices result of three controllers for the stochastic and seismic signal. It indicates that ABSMC achieves better performance than PID and SMC. The SMC greatly improves the tracking accuracy of the reference acceleration signal, and the M_e under stochastic signal and seismic signal decreases by 40.43% and 23.49%, respectively. The M_e, μ_e, and σ_e under the SMC are smaller than the PID because the SMC can handle the unmodeled disturbances and uncertainties to some extent under challenging working conditions. The σ_e of the stochastic signal reduces from 0.8012 to 0.2059, and the seismic signal from 0.6512 to 0.2153, confirming the importance of parameters adaption law.
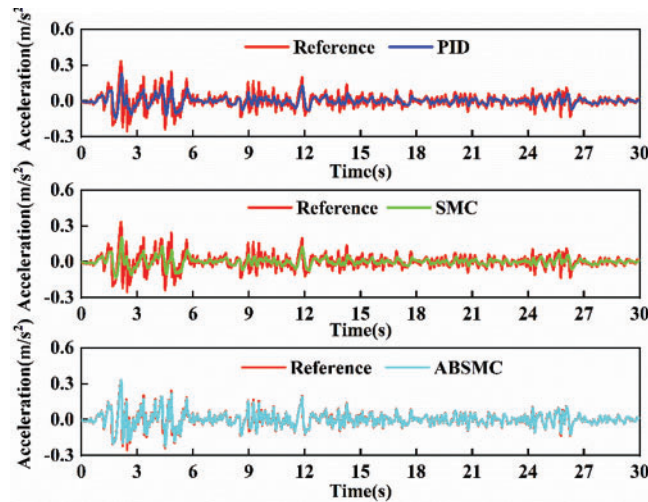
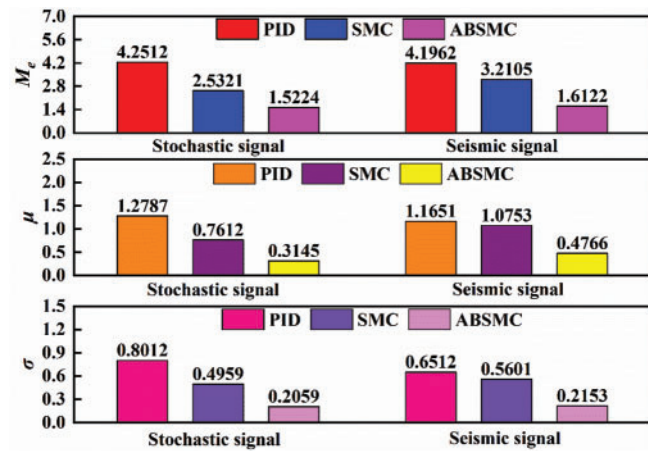**Figure 15:** Tracking trajectory of seismic acceleration motion

Figure 16: Comparison performance indices result of three controllers

The tracking trajectory of the step signal for three controllers is shown in Fig. 17. Large fluctuations occur in the initial stage of the PID, while the initial stage of SMC and ABSMC shows smooth tracking. The transient and steady-state performance indices of the step signal are listed in Table 5. ABSMC produces the highest tracking performance, and PID generates the worst tracking performance. The overshoot under step signal is reduced to 4.662% of ABSMC controller, down from 36.44% of PID controller. The steady-state error of the ABSMC controller is only 20% of that of the SMC controller, which illustrates the effectiveness of the adaptive control law. All results demonstrate that the developed ABSMC controller performs better than the other controllers.
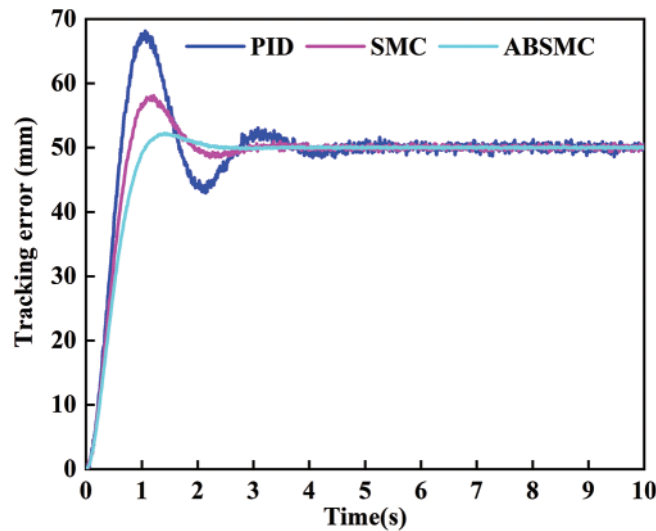
Figure 17: Tracking trajectory of step signal

Table 5: Transient and steady-state performance indices of step signal

Indices	Settling time (s)	Overshoot (%)	Steady-state error (mm)
PID	9.5764	36.44	0.4174
SMC	1.6705	16.09	0.2988
ABSMC	0.9209	4.662	0.0587

5 Conclusion

This study develops an ABSMC for hydraulic actuators with high-precision trajectory tracking control subjected to model uncertainties and disturbances. It first establishes the hydraulic actuator dynamic model and derives the corresponding state-space equation. Next, the ABSMC is designed to improve the system's robustness, where the adaptive law is employed to estimate unknown uncertainties. Finally, comparative experimental results verify the effectiveness of the proposed control scheme. Complex working conditions in the controller design will be considered for future work, such as hydraulic actuators with input saturation and state constraints. The limitation of this study is that the controller performance under different degrees of model uncertainty and dynamic interference is not further investigated.

Author Contributions: The authors confirm their contribution to the paper as follows: study conception and design: Zhenshuai Wan, Longwang Yue; system analysis and modeling: Zhenshuai Wan, Pu Zhao; controller and observer design: Zhenshuai Wan; platform construction and experimental design: Zhenshuai Wan; Yanfeng Wang; analysis and interpretation of results: Zhenshuai Wan, Yanfeng Wang; draft manuscript preparation: Zhenshuai Wan, Yanfeng Wang. All authors reviewed the results and approved the final version of the manuscript.

Availability of Data and Materials: The datasets generated and/or analyzed during this study are available from the corresponding author upon reasonable request.

Ethics Approval: Not applicable.

Conflicts of Interest: The authors have no conflicts of interest that could potentially influence the integrity, objectivity, or impartiality of the research presented in this article.

References

1. Zhang J, Liu J, Ding F. Collaborative optimization design framework for hierarchical filter barrier control suspension system with projection adaptive tracking hydraulic actuator. Nonlin Dynam. 2022;108(4):3417–34. doi:10.1007/s11071-022-07374-x.

2. Guo Q, Chen ZL. Neural adaptive control of single-rod electrohydraulic system with lumped uncertainty. Mech Syst Signal Pr. 2021;146(2):106869. doi:10.1016/j.ymssp.2020.106869.

3. Yuan S, Deng W, Liang X, Yao J, Yang G. Nonlinear robust adaptive precision motion control of motor servo systems with unknown actuator backlash compensation. ISA Trans. 2023;137(1):349–57. doi:10.1016/j.isatra.2023.02.002.

4. Na J, Wang SB, Liu YJ, Huang YB, Ren XM. Finite-time convergence adaptive neural network control for nonlinear servo systems. IEEE Trans Cybern. 2020;50(6):2568–79. doi:10.1109/TCYB.2019.2893317.

5. Wang SB, Na J, Ren XM, Yu HS, Yu JP. Unknown input observer-based robust adaptive funnel motion control for nonlinear servomechanisms. Int J Robust Nonlin. 2018;28(18):6163–79. doi:10.1002/rnc.4368.

6. Van M, Do XP, Mavrovouniotis M. Self-tuning fuzzy PID-nonsingular fast terminal sliding mode control for robust fault tolerant control of robot manipulators. ISA Trans. 2020;96(4):60–8. doi:10.1016/j.isatra.2019.06.017.

7. Guo Q, Li XC, Zuo ZY, Shi Y, Jiang D. Quasi-synchronization control of multiple electrohydraulic actuators with load disturbance and uncertain parameters. IEEE/ASME Trans Mechatron. 2021;26(4):2048–58. doi:10.1109/TMECH.2020.3030032.

8. Yang XB, Zheng XL, Chen YH. Position tracking control law for an electro-hydraulic servo system based on back-stepping and extended differentiator. IEEE/ASME Trans Mechatron. 2018;23(1):132–40. doi:10.1109/TMECH.2017.2746142.

9. Jing CH, Xu HG, Jiang JH. Dynamic surface disturbance rejection control for electro-hydraulic load simulator. Mech Syst Signal Pr. 2019;134:106293. doi:10.1016/j.ymssp.2019.106293.

10. Liu L, Zhao W, Liu YJ, Tong S, Wang YY. Adaptive finite-time neural network control of nonlinear systems with multiple objective constraints and application to electromechanical system. IEEE Trans Neur Net Lear. 2021;32(12):5416–26. doi:10.1109/TNNLS.2020.3027689.

11. Na J, Ren XM, Herrmann G, Qiao Z. Adaptive neural dynamic surface control for servo systems with unknown dead-zone. Control Eng Pract. 2011;19(11):1328–43. doi:10.1016/j.conengprac.2011.07.005.

12. Niu B, Duan P, Li J, Li X. Adaptive neural tracking control scheme of switched stochastic nonlinear pure-feedback nonlower triangular systems. IEEE Trans Syst Man Cybern: Syst. 2021;51(2):975–86. doi:10.1109/TSMC.2019.2894745.

13. Qiao L, Zhang WD. Trajectory tracking control of AUVs via adaptive fast nonsingular integral terminal sliding mode control. IEEE Trans Ind Inform. 2020;16(2):1248–58. doi:10.1109/TII.2019.2949007.

14. Jin M, Kang SH, Chang PH, Lee J. Robust control of robot manipulators using inclusive and enhanced time delay control. IEEE-ASME Trans Mech. 2017;22(5):2141–52. doi:10.1109/TMECH.2017.2718108.

15. Kim BS, Yoo SJ. Approximation-based adaptive tracking control of nonlinear pure-feedback systems with time-varying output constraints. INT J Control Autom. 2015;13(2):257–65. doi:10.1007/s12555-014-0084-6.

16. Yan S, Sun WC, He FH, Yao JY. Adaptive fault detection and isolation for active suspension systems with model uncertainties. IEEE Trans Reliab. 2019;68(3):927–37. doi:10.1109/TR.2018.2868949.

17. Liu W, Lim C-C, Shi P, Xu S. Back-stepping fuzzy adaptive control for a class of quantized nonlinear systems. IEEE Trans Fuzzy Syst. 2017;25(5):1090–101. doi:10.1109/TFUZZ.2016.2598360.

18. Huang YB, Na J, Wu X, Gao GB. Approximation-free control for vehicle active suspensions with hydraulic actuator. IEEE Trans Ind Electron. 2018;65(9):7258–67. doi:10.1109/TIE.2018.2798564.

19. Razzaghian A, Moghaddam RK, Pariz N. Fractional-order nonsingular terminal sliding mode control via a disturbance observer for a class of nonlinear systems with mismatched disturbances. J Vib Control. 2021;27(1–2):140–51. doi:10.1177/1077546320925263.

20. Xu N, Liu X, Li Y, Zong G, Zhao X, Wang H. Dynamic event-triggered control for a class of uncertain strict-feedback systems via an improved adaptive neural networks back-stepping approach. IEEE Trans Autom Sci Eng. 2024;1–10. doi:10.1109/TASE.2024.3374522.

21. Zhang MJ, Liu X, Yin BJ, Liu WX. Adaptive terminal sliding mode based thruster fault tolerant control for underwater vehicle in time-varying ocean currents. J Frank Inst. 2015;352(11):4935–61. doi:10.1016/j.jfranklin.2015.08.009.

22. Li C, Chen Z, Yao B. Identification and adaptive robust precision motion control of systems with nonlinear friction. Nonlin Dynam. 2019;95(2):995–1007. doi:10.1007/s11071-018-4610-6.

23. Essa MEM, Aboelela MAS, Hassan MAM, Abdrabbo SM. Model predictive force control of hardware implementation for electro-hydraulic servo system. Trans Inst Meas Control. 2019;41(5):1435–46. doi:10.1177/0142331218784118.

24. Zhao H, Zhao N, Zong G, Zhao X, Xu N. Sliding-mode surface-based approximate optimal control for nonlinear multiplayer Stackelberg-Nash games via adaptive dynamic programming. Commun Nonlin Sci. 2024;132(7):107928. doi:10.1016/j.cnsns.2024.107928.

25. Guo K, Li M, Shi W, Pan Y. Adaptive tracking control of hydraulic systems with improved parameter convergence. IEEE Trans Ind Electron. 2022;69(7):7140–50. doi:10.1109/TIE.2021.3101006.

26. Guo Q, Zhang Y, Celler BG, Su SW. Back-stepping control of electro-hydraulic system based on extended-state-observer with plant dynamics largely unknown. IEEE Trans Ind Electron. 2016;63(11):6909–20. doi:10.1109/TIE.2016.2585080.

27. Cheng C, Liu SY, Wu HZ. Sliding mode observer-based fractional-order proportional-integral-derivative sliding mode control for electro-hydraulic servo systems. Proc Inst Mech Eng Part C: J Mech Eng Sci. 2020;234(10):1887–98. doi:10.1177/0954406220903337.

28. Zhuang HX, Sun QL, Chen ZQ, Jiang YX. Back-stepping sliding mode control for pressure regulation of oxygen mask based on an extended state observer. Automatica. 2020;119(9):109106. doi:10.1016/j.automatica.2020.109106.

29. Chen Z, Guo Q, Li T, Yan Y, Jiang D. Gait prediction and variable admittance control for lower limb exoskeleton with measurement delay and extended-state-observer. IEEE Trans Neur Net Lear. 2022;34(11):1–14.

30. Asl RM, Hagh YS, Anavatti S, Handroos H. Adaptive finite integral non-singular terminal synergetic control of nth-order nonlinear systems. Mech Syst Signal Pr. 2020;142(5):106789. doi:10.1016/j.ymssp.2020.106789.

31. Zhao J, Na J, Gao GB. Robust tracking control of uncertain nonlinear systems with adaptive dynamic programming. Neurocomputing. 2022;471(6):21–30. doi:10.1016/j.neucom.2021.10.081.

32. Yang CG, Jiang YM, He W, Na J, Li ZJ, Xu B. Adaptive parameter estimation and control design for robot manipulators with finite-time convergence. IEEE Trans Ind Electron. 2018;65(10):8112–23. doi:10.1109/TIE.2018.2803773.

33. Palli G, Strano S, Terzo M. Sliding-mode observers for state and disturbance estimation in electro-hydraulic systems. Control Eng Pract. 2018;74(9):58–70. doi:10.1016/j.conengprac.2018.02.007.

34. Park JH, Kim SH, Park TS. Output-feedback adaptive neural controller for uncertain pure-feedback nonlinear systems using a high-order sliding mode observer. IEEE Trans Neur Net Lear. 2019;30(5):1596–601. doi:10.1109/TNNLS.2018.2861942.

35. Xin C, Li YX, Ahn CK. Adaptive neural asymptotic tracking of uncertain non-strict feedback systems with full-state constraints via command filtered technique. IEEE Trans Neur Net Lear. 2022;34(10):1–6.